# Supplementary Information

## Bent 1,10-phenanthroline ligands within octahedral complexes constructed around a $TiO_4N_2$ core

Matthieu Scarpi-Luttenauer,a Loris Geminiani,a Pauline Lebrun,a Nathalie Kyritsakas,b Alain Chaumont,a Marc Henry,a Pierre Mobian*,a

a) Laboratoire de Chimie Moléculaire de l'Etat Solide, UMR 7140 UDS-CNRS, Université de Strasbourg, 4 rue Blaise Pascal, F-67000 Strasbourg, France.

b) Laboratoire de Tectonique Moléculaire, UMR 7140 UDS-CNRS, Université de Strasbourg, 4 rue Blaise Pascal, F-67000 Strasbourg, France.

c) Laboratoire de Modélisation et Simulations Moléculaires, UMR 7140 UDS-CNRS, Université de Strasbourg, 4 rue Blaise Pascal, F-67000 Strasbourg, France.

* Email: mobian@unistra.fr

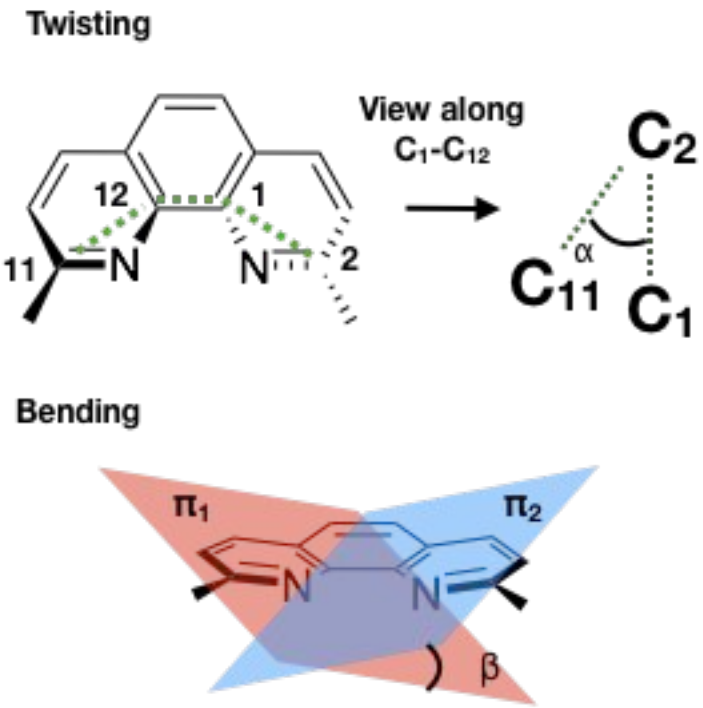

Scheme 1: $\alpha$ and $\beta$ angles used to evaluate the distortion of the phenanthroline ligands.

## 1. NMR Spectra

For the superpositions: the spectra of the designated complexes (black) and their corresponding ligand (red) are stacked. Shifting of the proton resonances on the 2,9-poisitions for the non-substituted ligands or the ending methyl protons for the alkyl-substituted phenanthrolines is shown by an arrow.

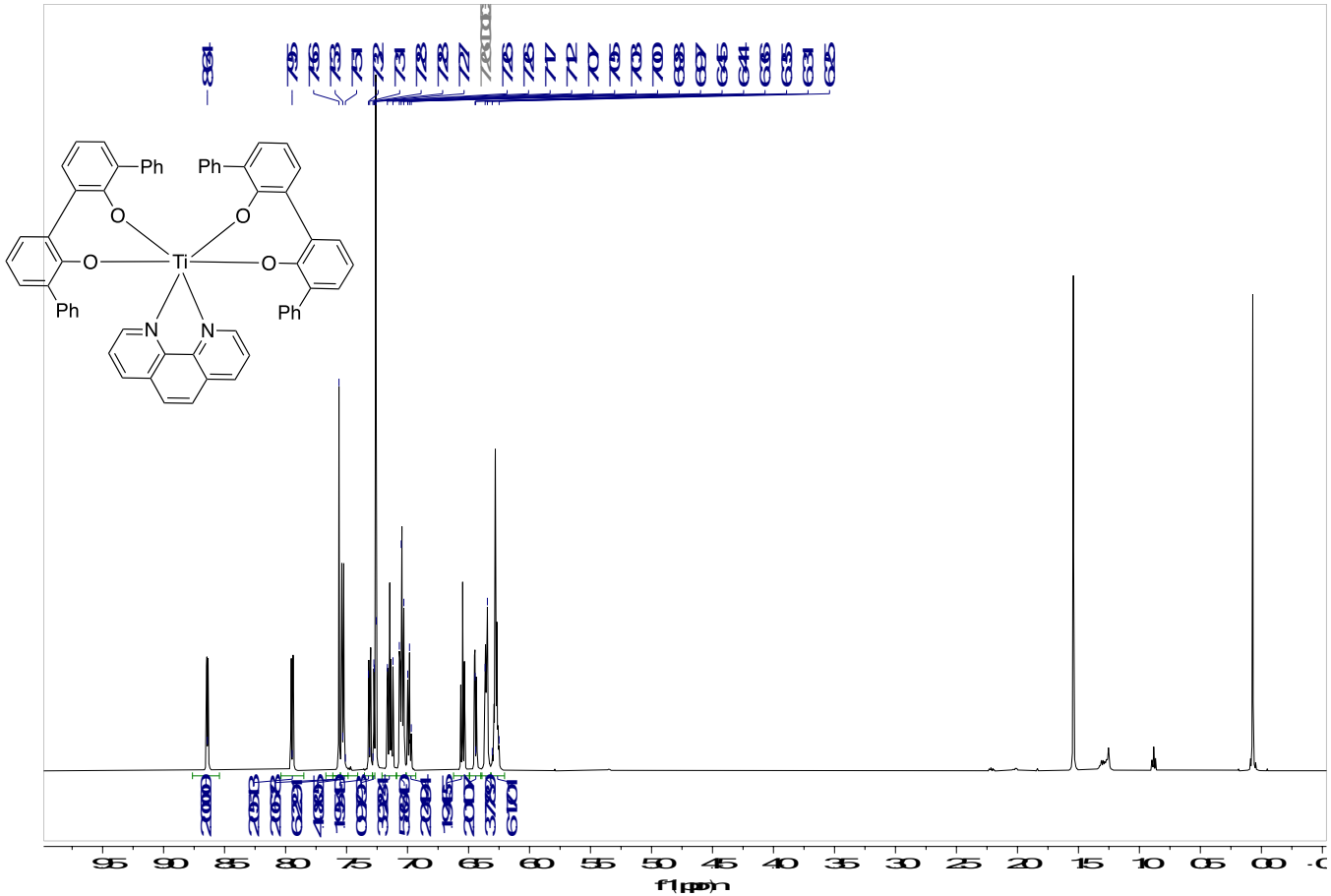


Figure S1: $^{1}H$ NMR spectrum of [Ti(1)$_2$(**2a**)] ($CDCl_3$, 500 MHz)

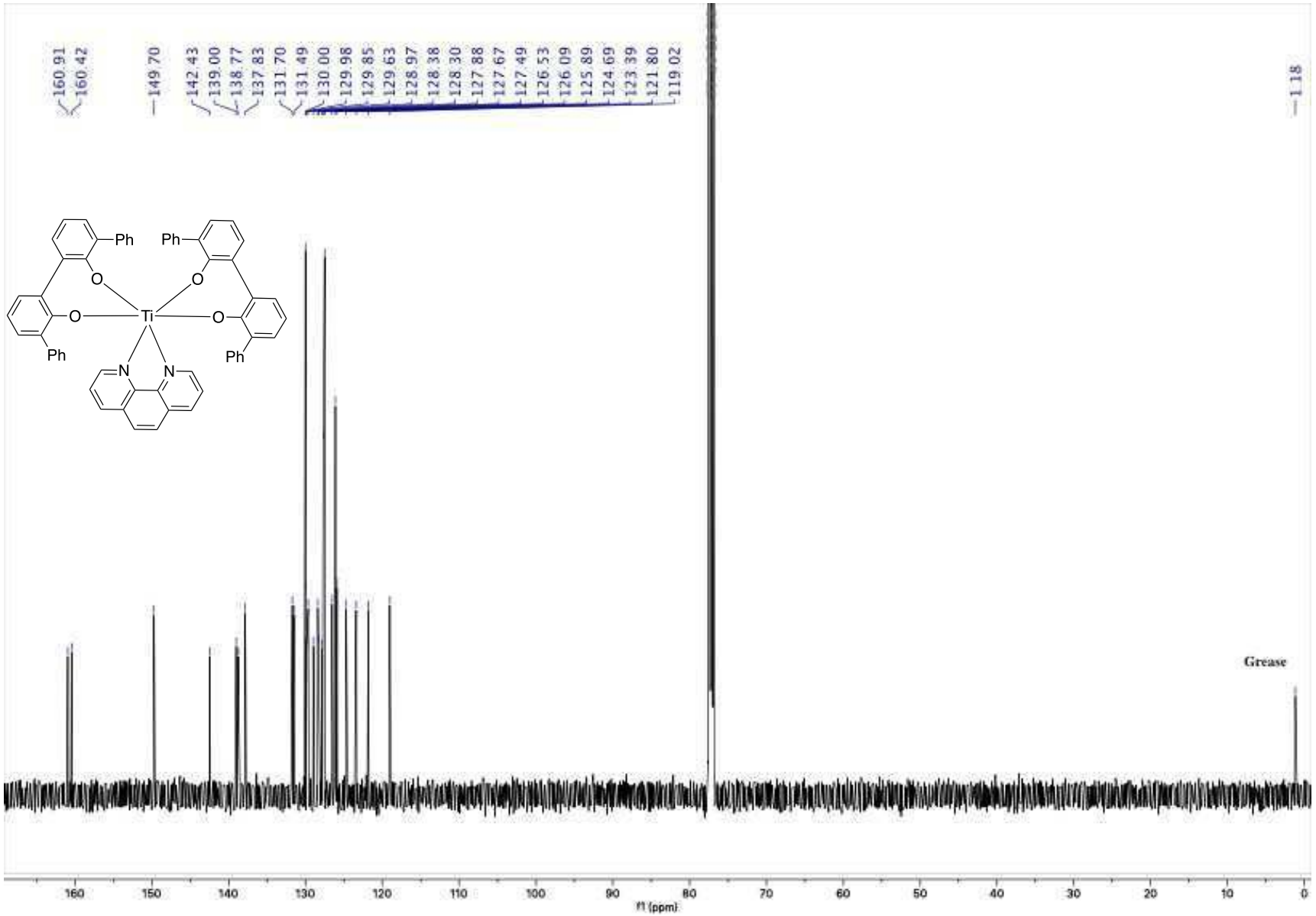


Figure S2: $^{13}C\{^{1}H\}$ NMR spectrum of [Ti(1)$_2$(**2a**)] ($CDCl_3$, 125 MHz)

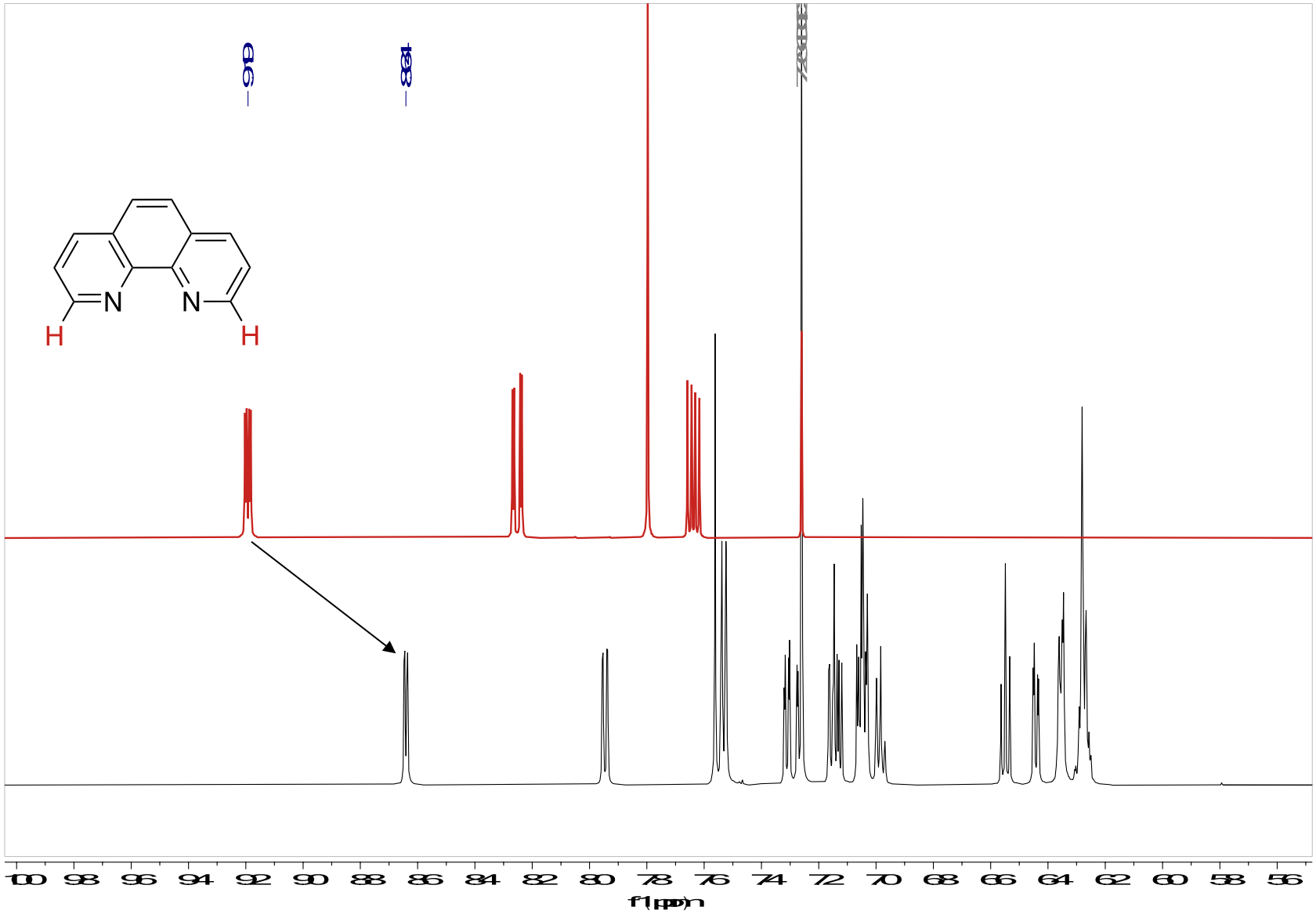


Figure S3: Superposition of the $^{1}H$ NMR spectra of **2a** (top) and [Ti(1)$_2$**(2a)**] (bottom) ($CDCl_3$, 500 MHz)

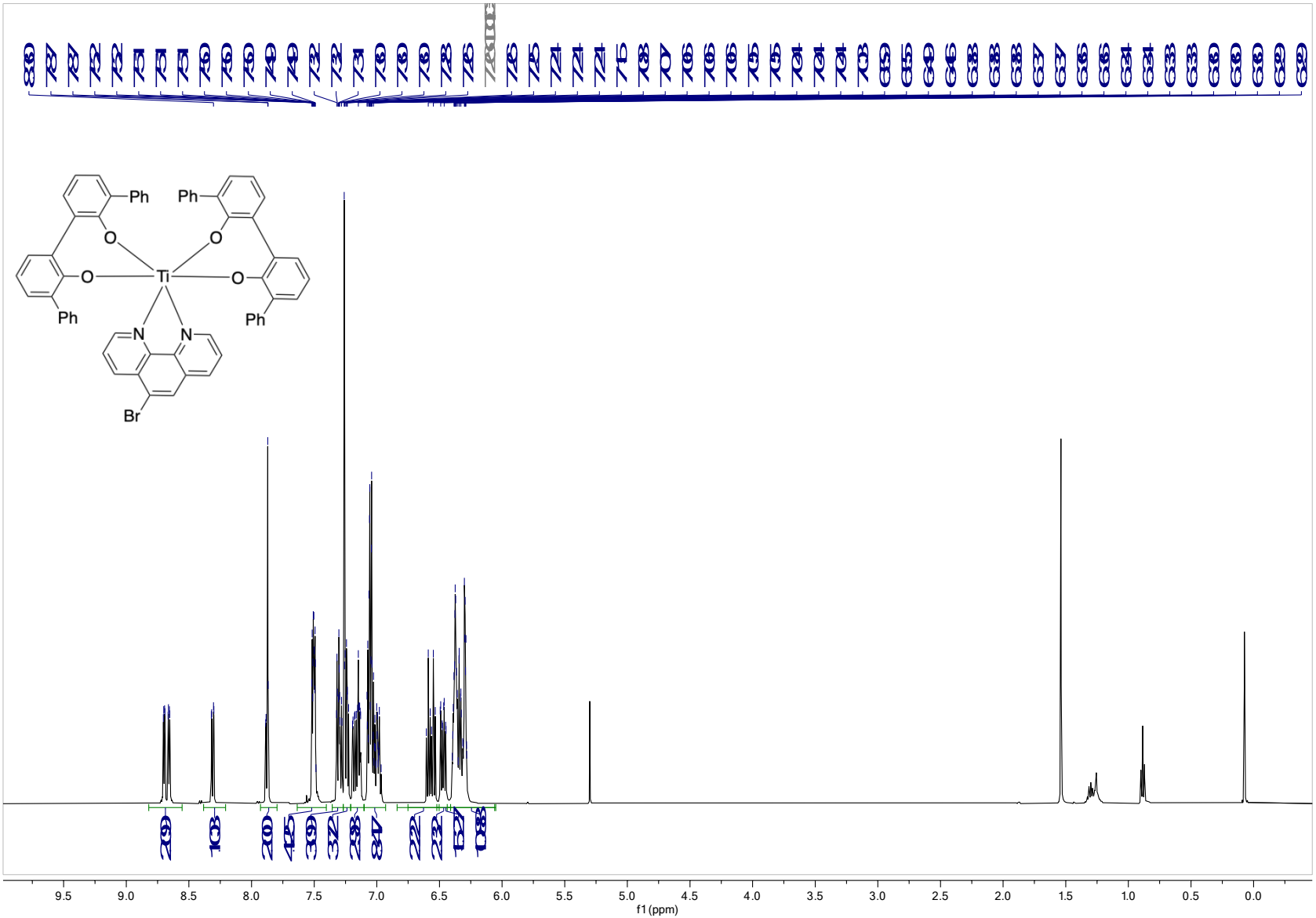


Figure S4: $^{1}H$ NMR spectrum of [Ti(1)$_2$(**2b**)] ($CDCl_3$, 500 MHz)

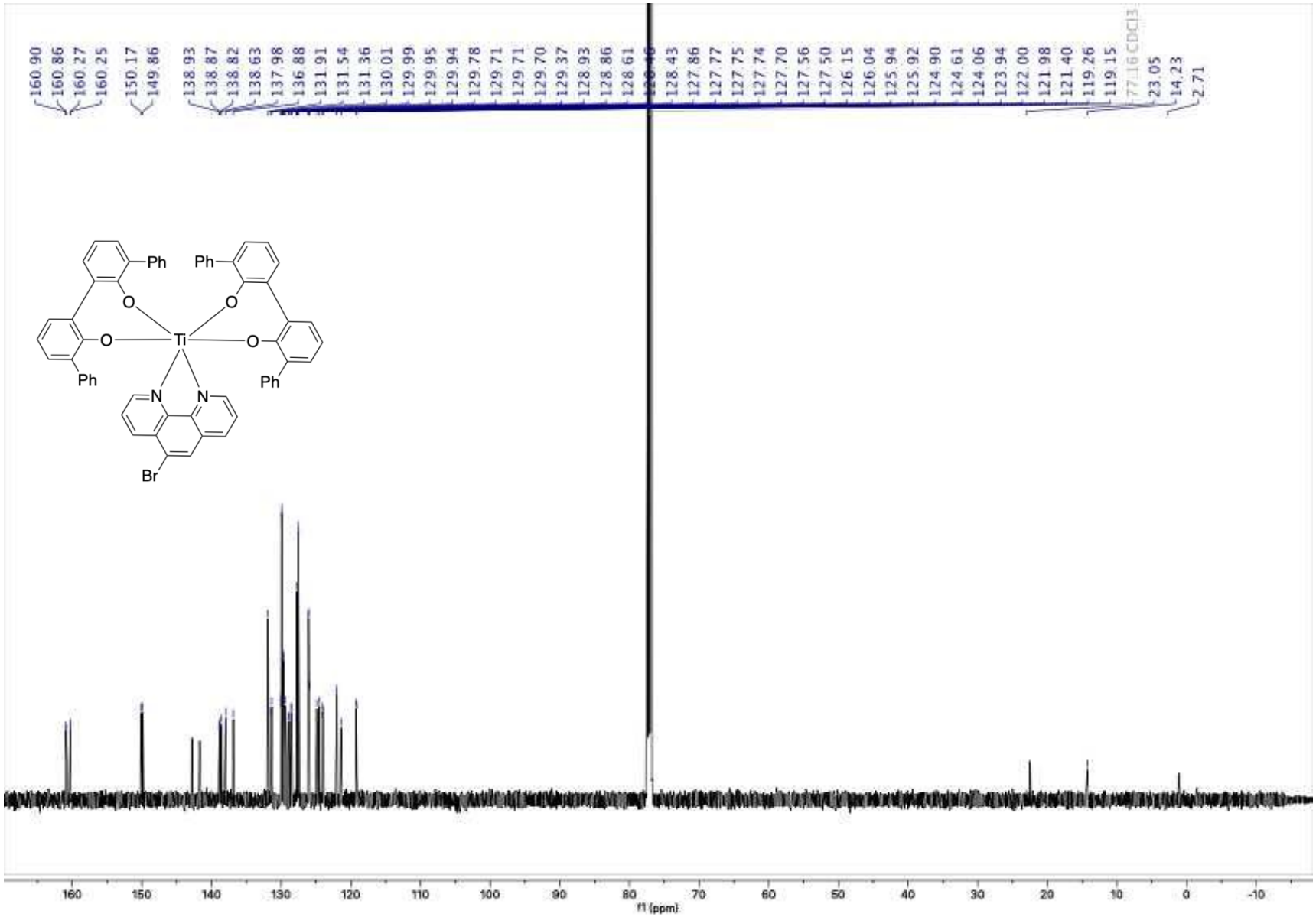


Figure S5: $^{13}C\{^{1}H\}$ NMR spectrum of [Ti(1)$_2$(**2b**)] ($CDCl_3$, 125 MHz)

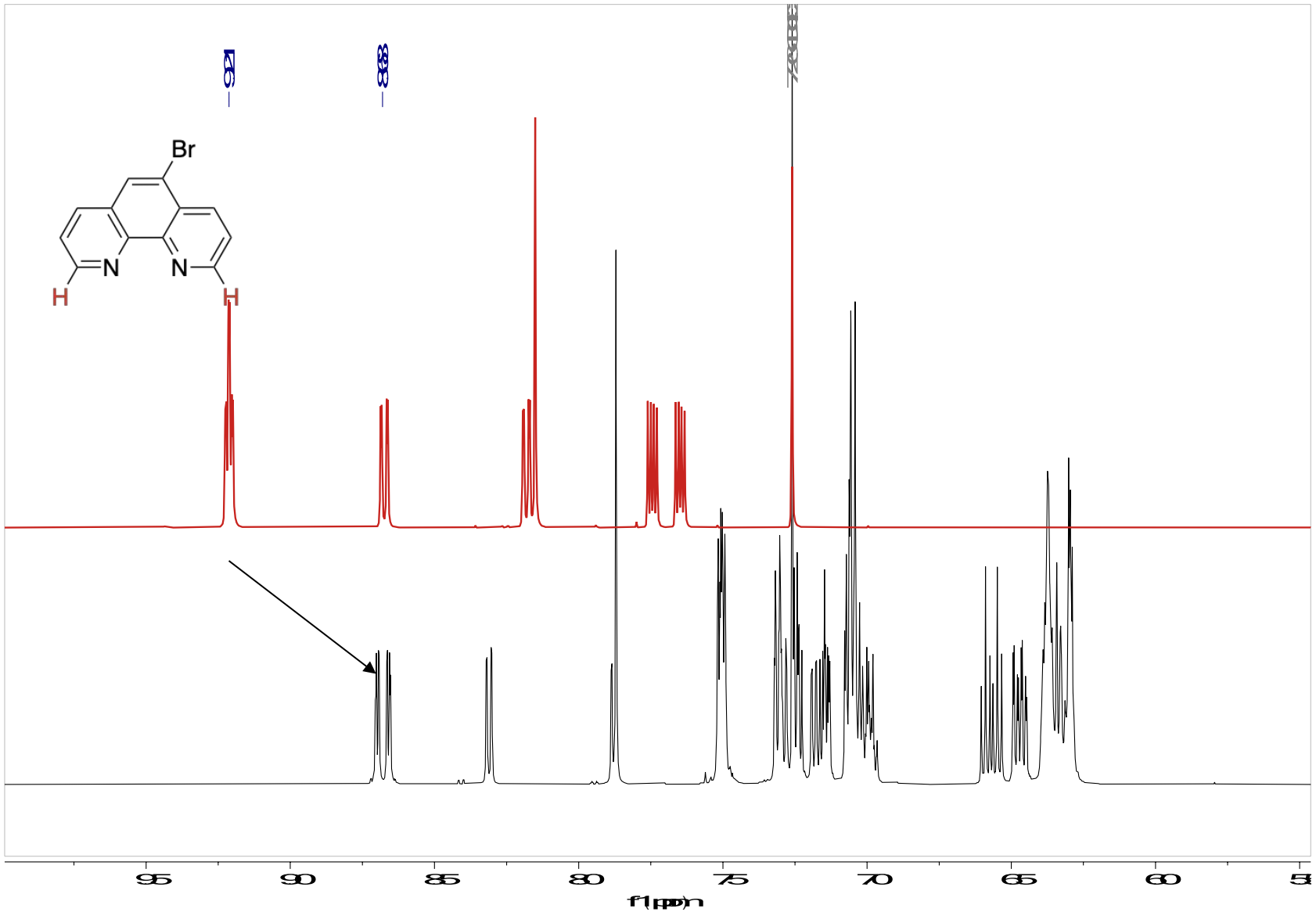


Figure S6: Superposition of the $^{1}H$ NMR spectra of **2b (top)** and [Ti(1)$_2$(**2b)**] (bottom) ($CDCl_3$, 500 MHz)

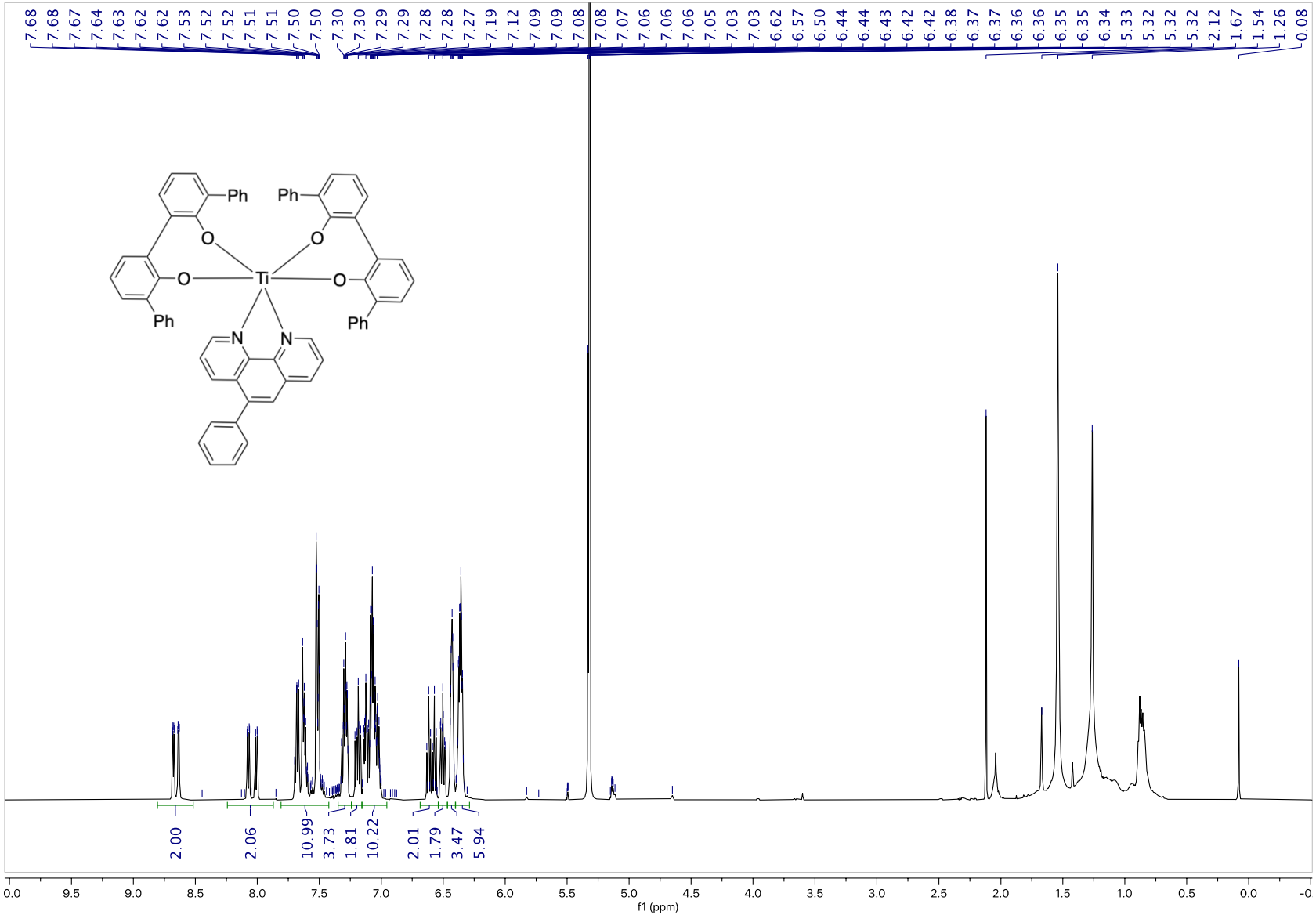


Figure S7: $^{1}$H NMR spectrum of [Ti(1)$_2$(**2c**)] ($CD_2Cl_2$, 500 MHz)

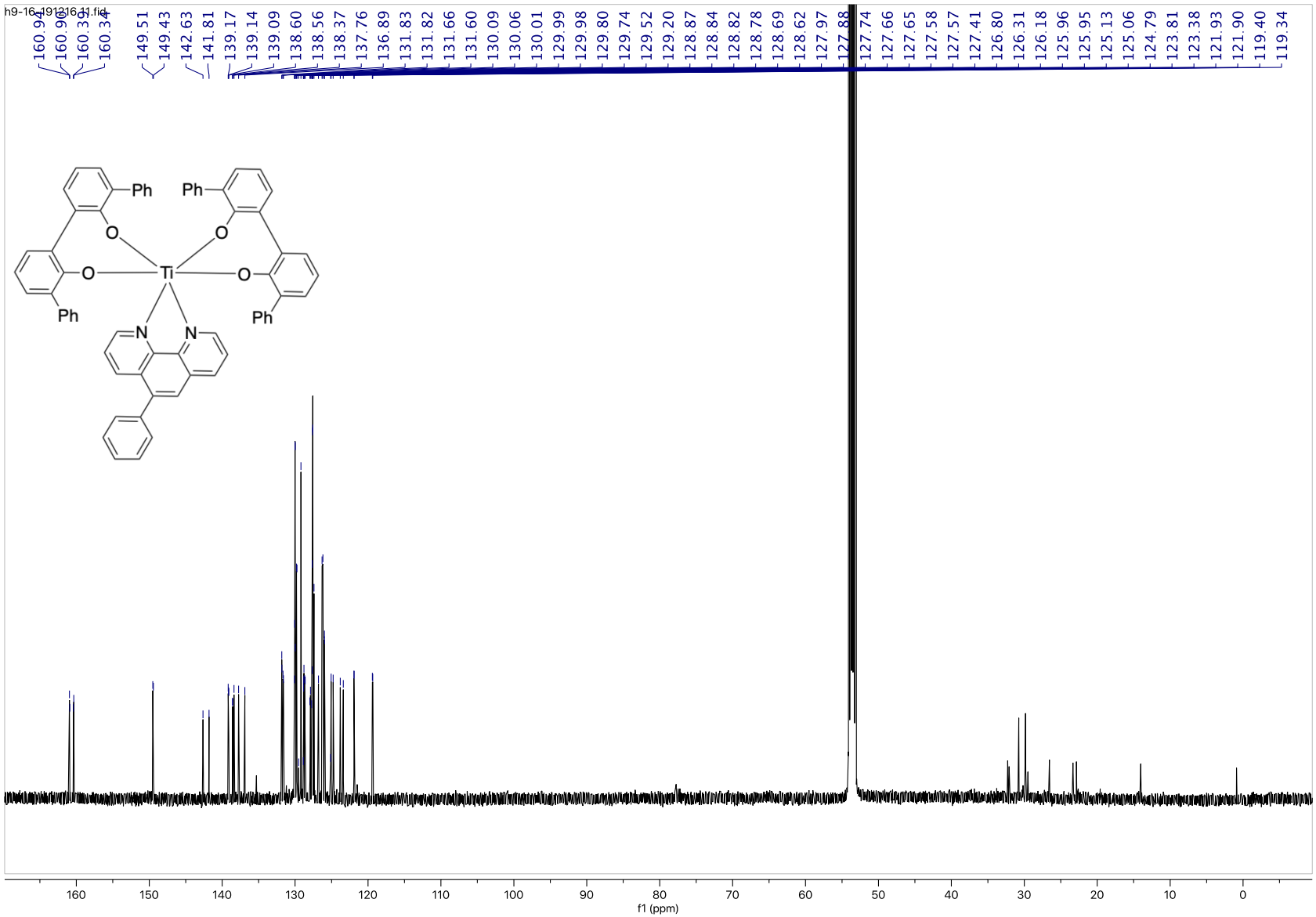


Figure S8: $^{13}C\{^{1}H\}$ NMR spectrum of [Ti(1)$_2$(**2c**)] ($CD_2Cl_2$, 125 MHz)

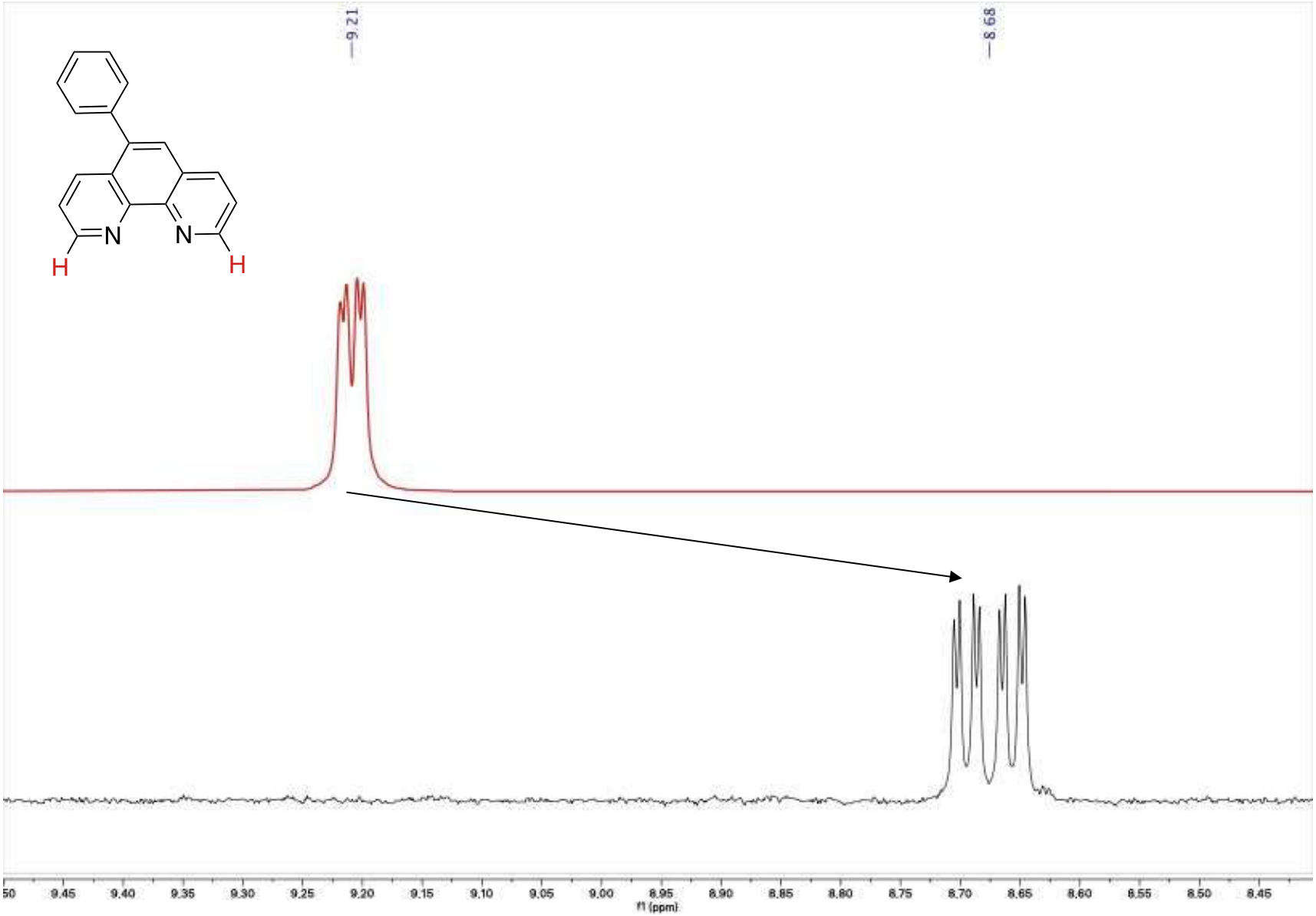


Figure S9: Superposition of the $^{1}H$ NMR spectra of **2c** (top) and [Ti(1)$_2$(**2c**)] (bottom) (selected region) ($CDCl_3$, 500 MHz)

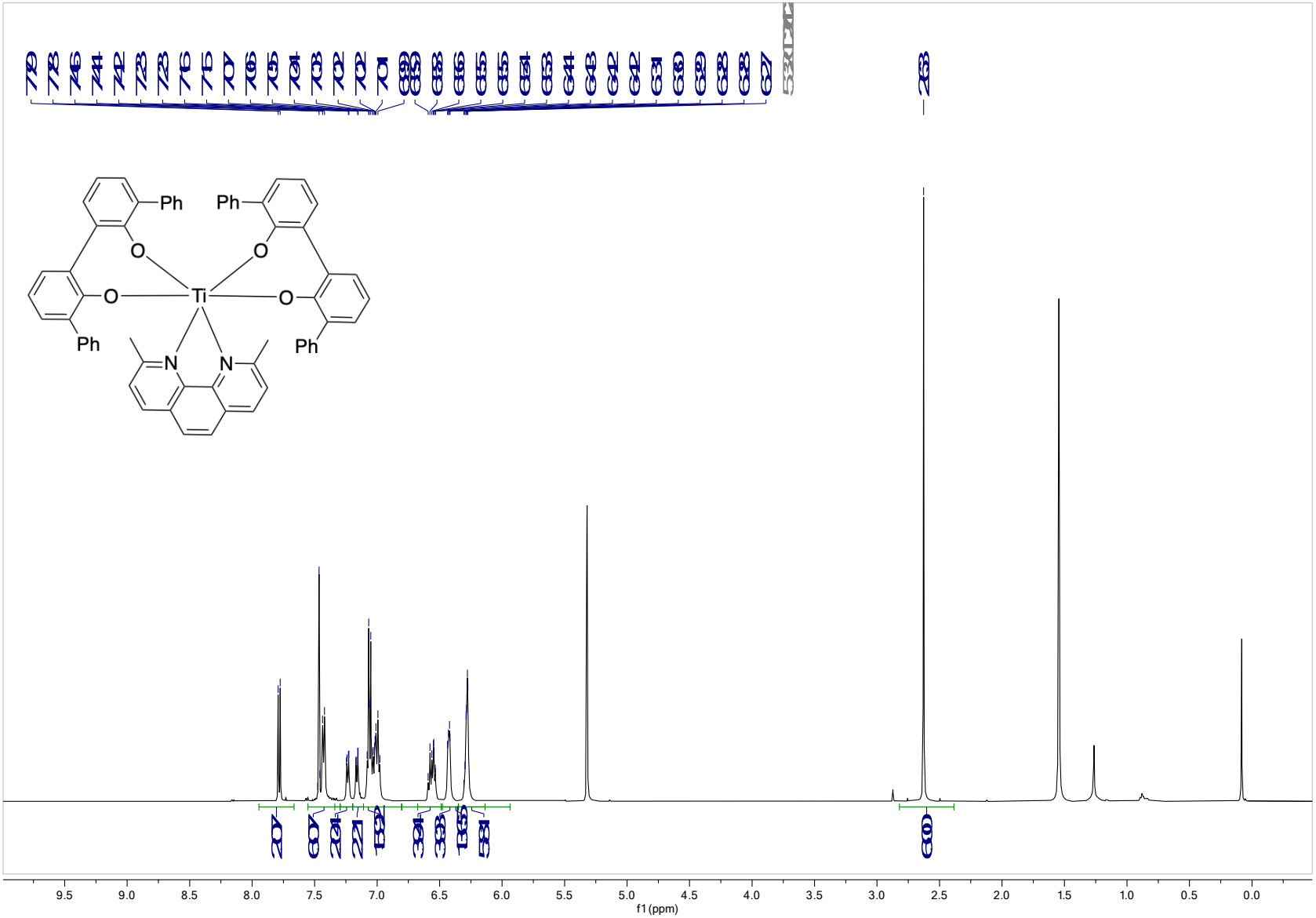


Figure S10: $^{1}H$ NMR spectrum of [Ti(1)$_2$(**2d**)] ($CD_2Cl_2$, 500 MHz)

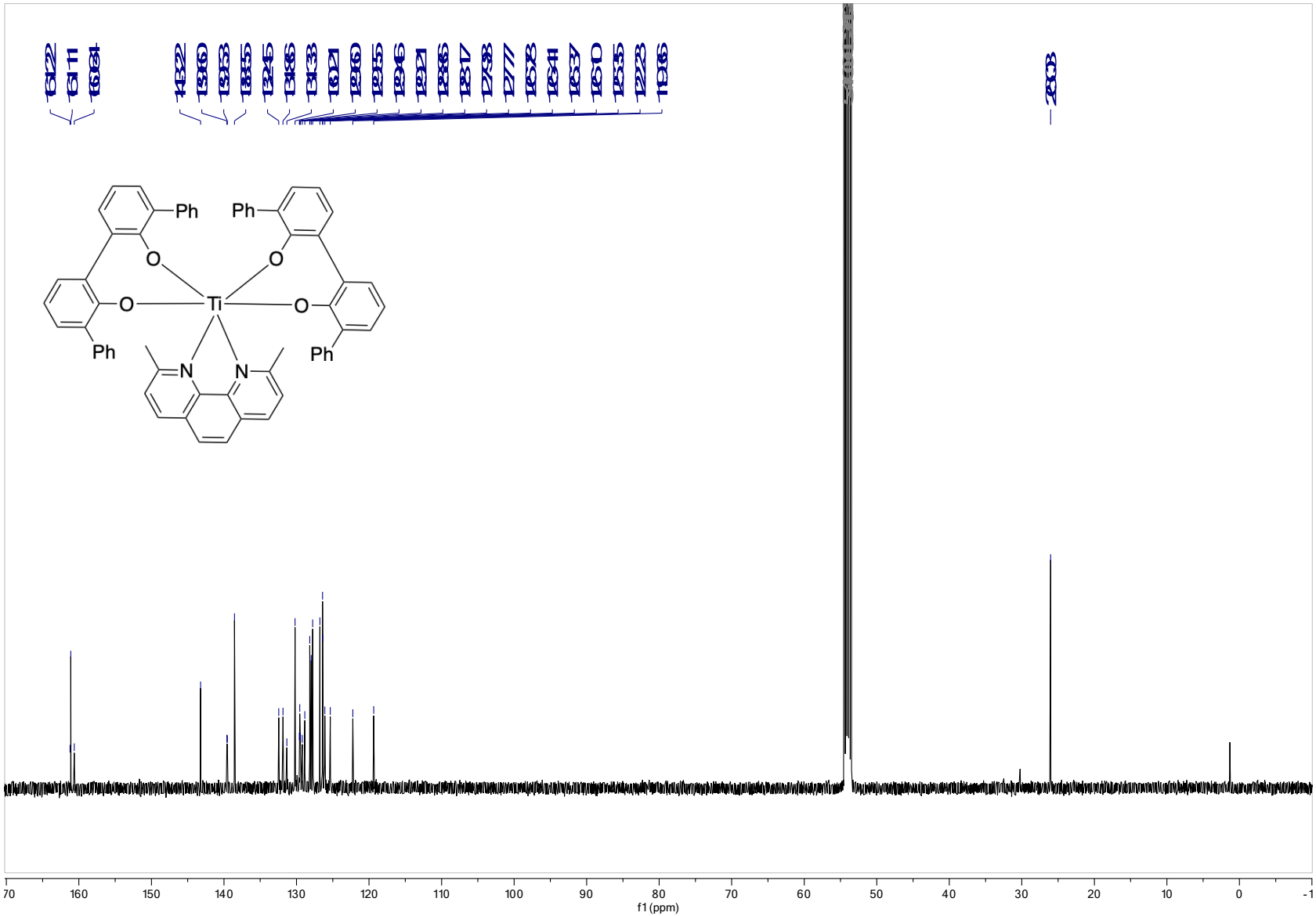


Figure S11: $^{13}C\{^{1}H\}$ NMR spectrum of [Ti(1)$_2$(**2d**)] ($CD_2Cl_2$, 125 MHz)

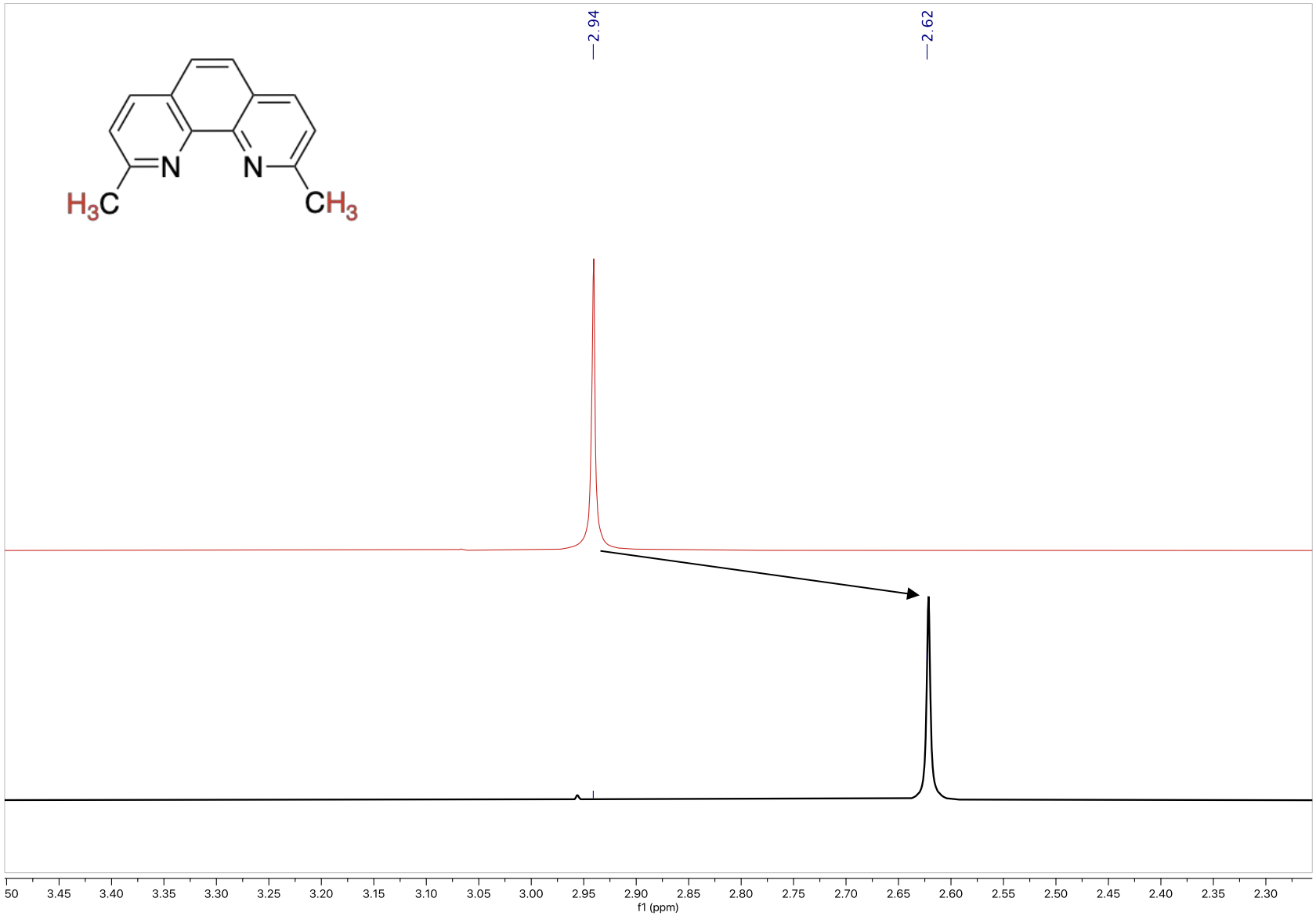


Figure S12: Superposition of the $^{1}$H NMR spectra of **2d** (top) and [Ti(1)$_2$(**2d**)] (bottom) ($CDCl_3$, 500 MHz)

Figure S13: $^{1}H$ NMR spectrum of [Ti(1)$_2$(**2e**)] ($CD_2Cl_2$, 500 MHz). It should be noted that an impurity (≈ 5 %) contaminates the sample. This impurity is assigned to the free ligand (see Figure S15).

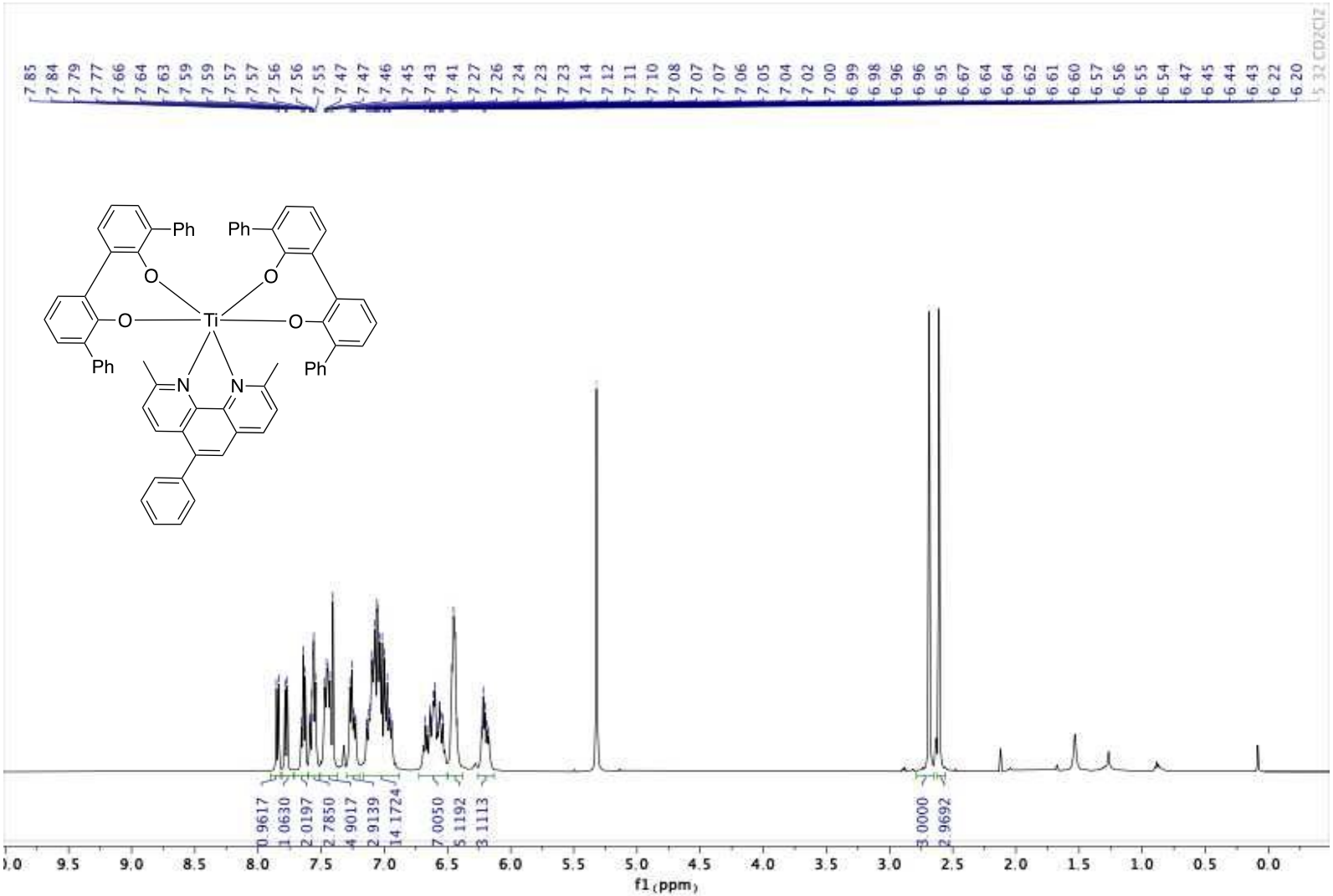

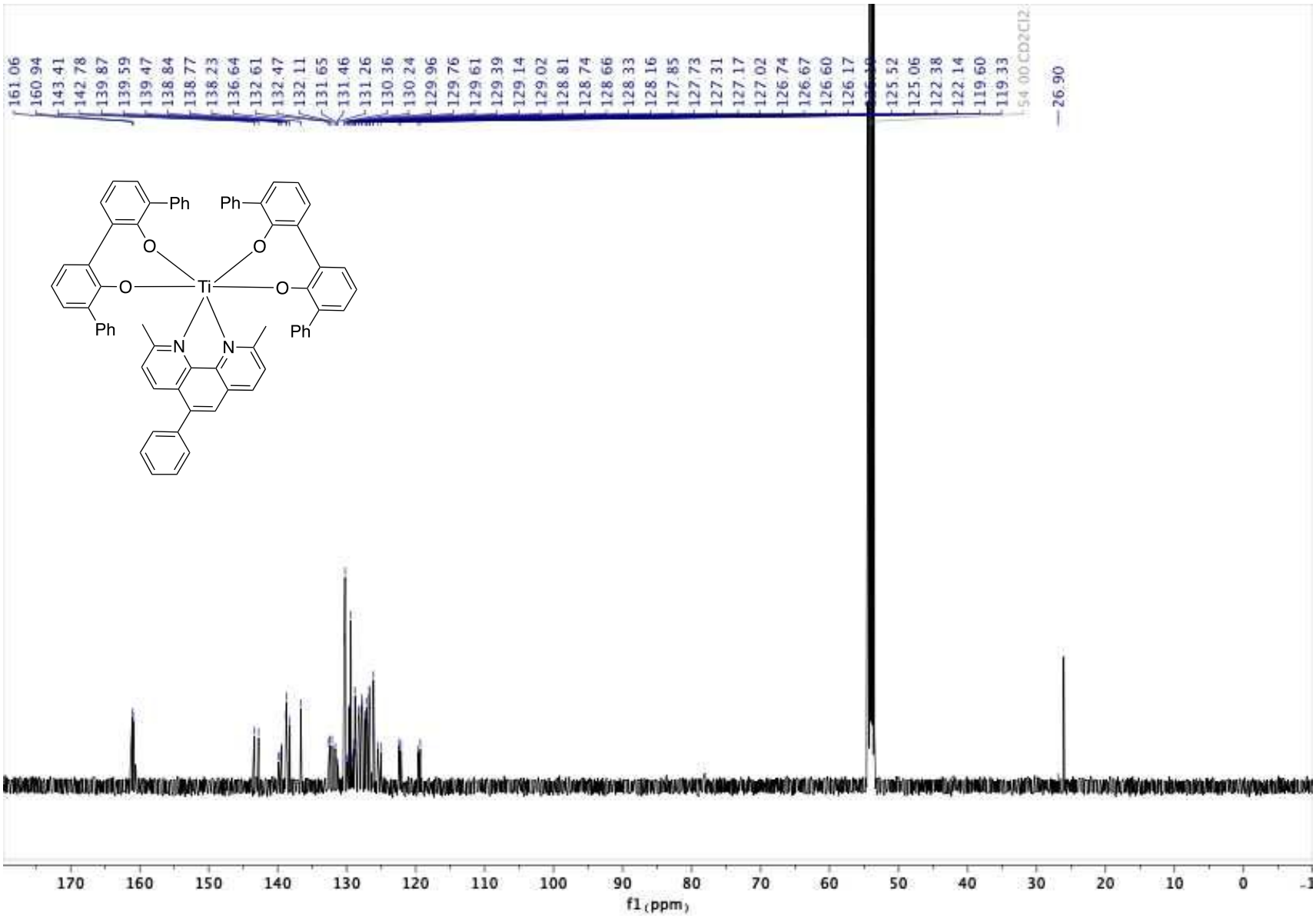


Figure S14: $^{13}C\{^{1}H\}$ NMR spectrum of [Ti(1)$_2$(**2e**)] ($CDCl_3$, 125 MHz)

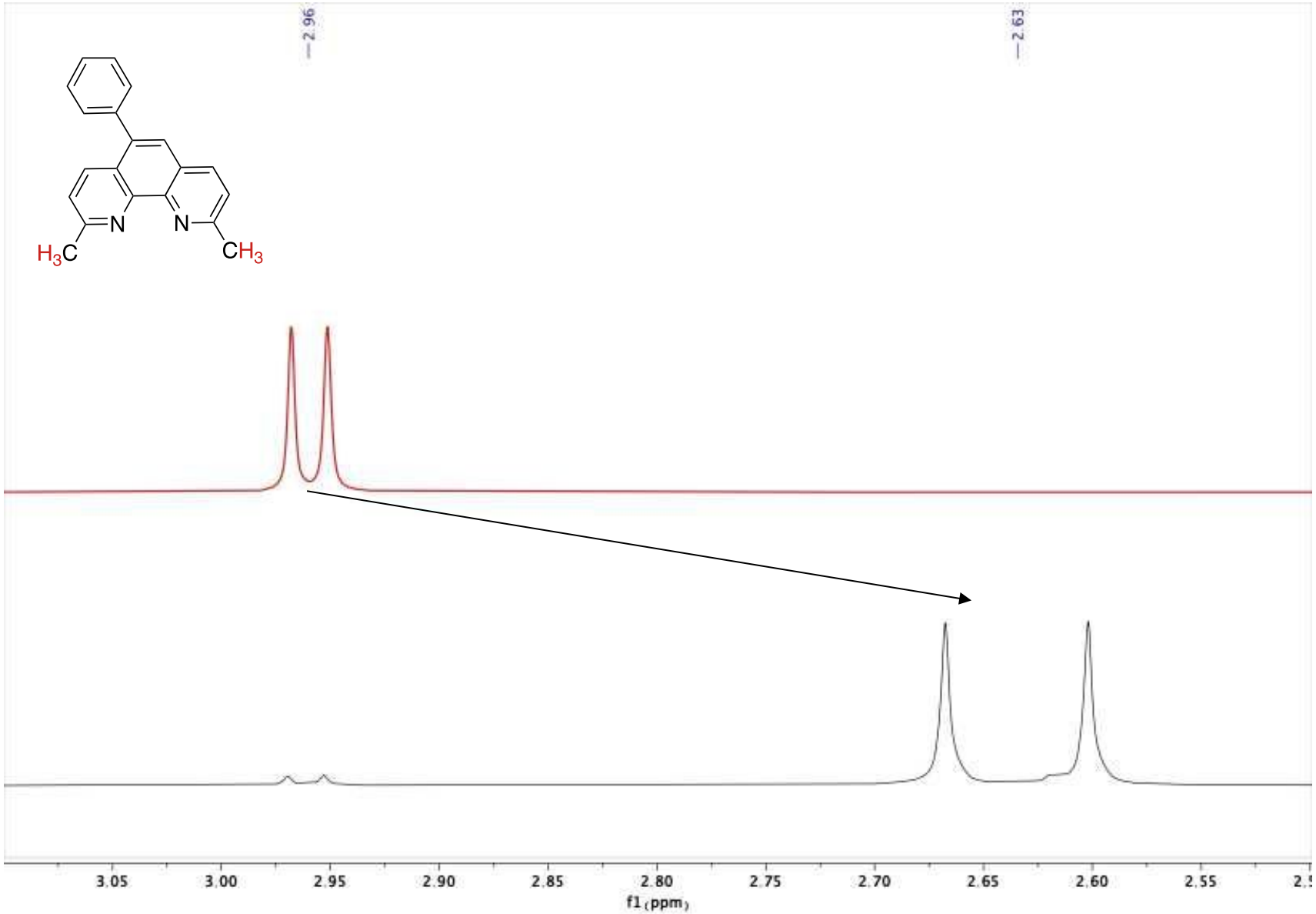


Figure S15: Superposition of the $^{1}H$ NMR spectra of **2e** (top) and [Ti(1)$_2$(**2e**)] (bottom) ($CDCl_3$, 500 MHz)

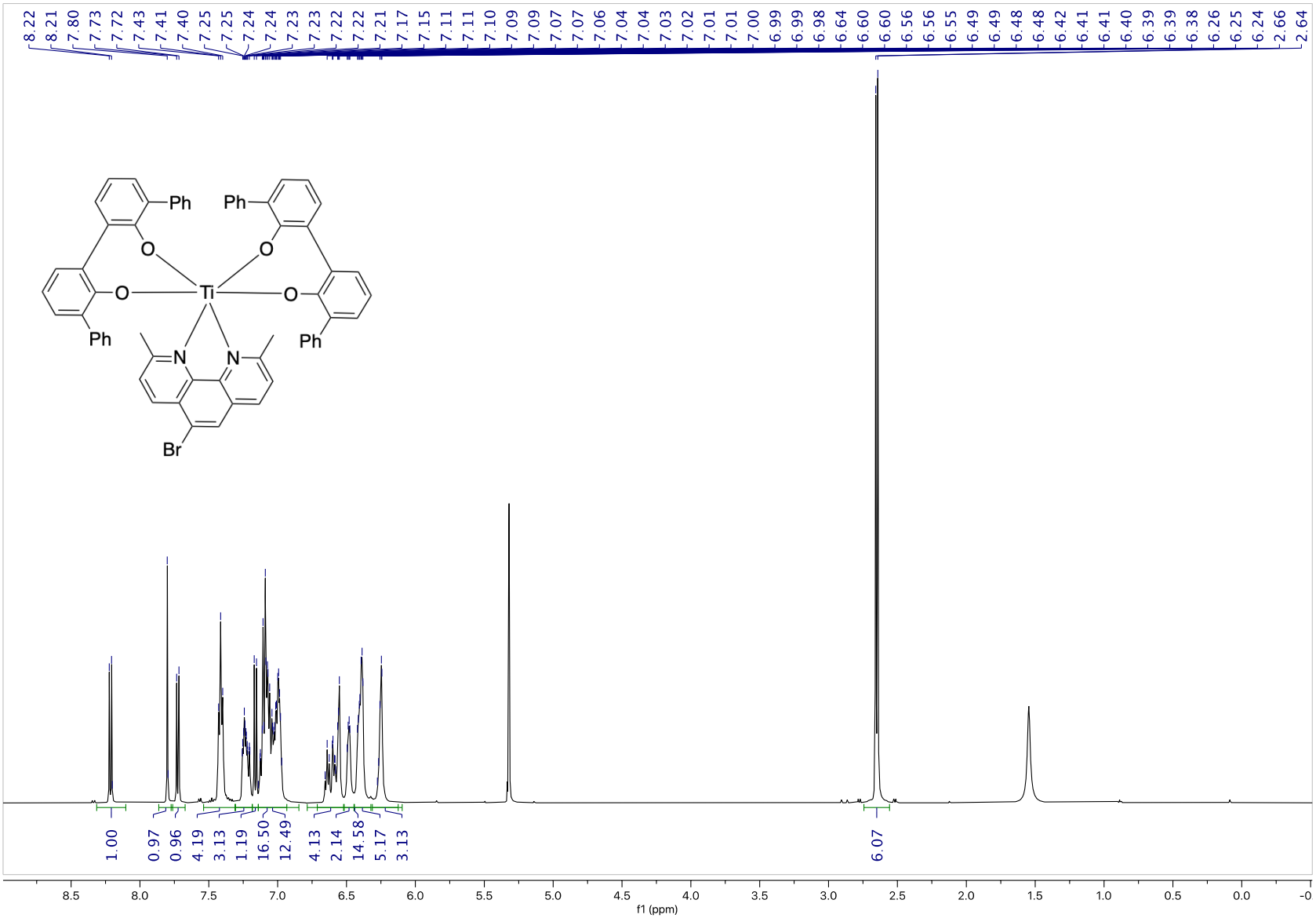


Figure S16: $^{1}H$ NMR spectrum of [Ti(1)$_2$(**2f**)] ($CDCl_3$, 500 MHz)

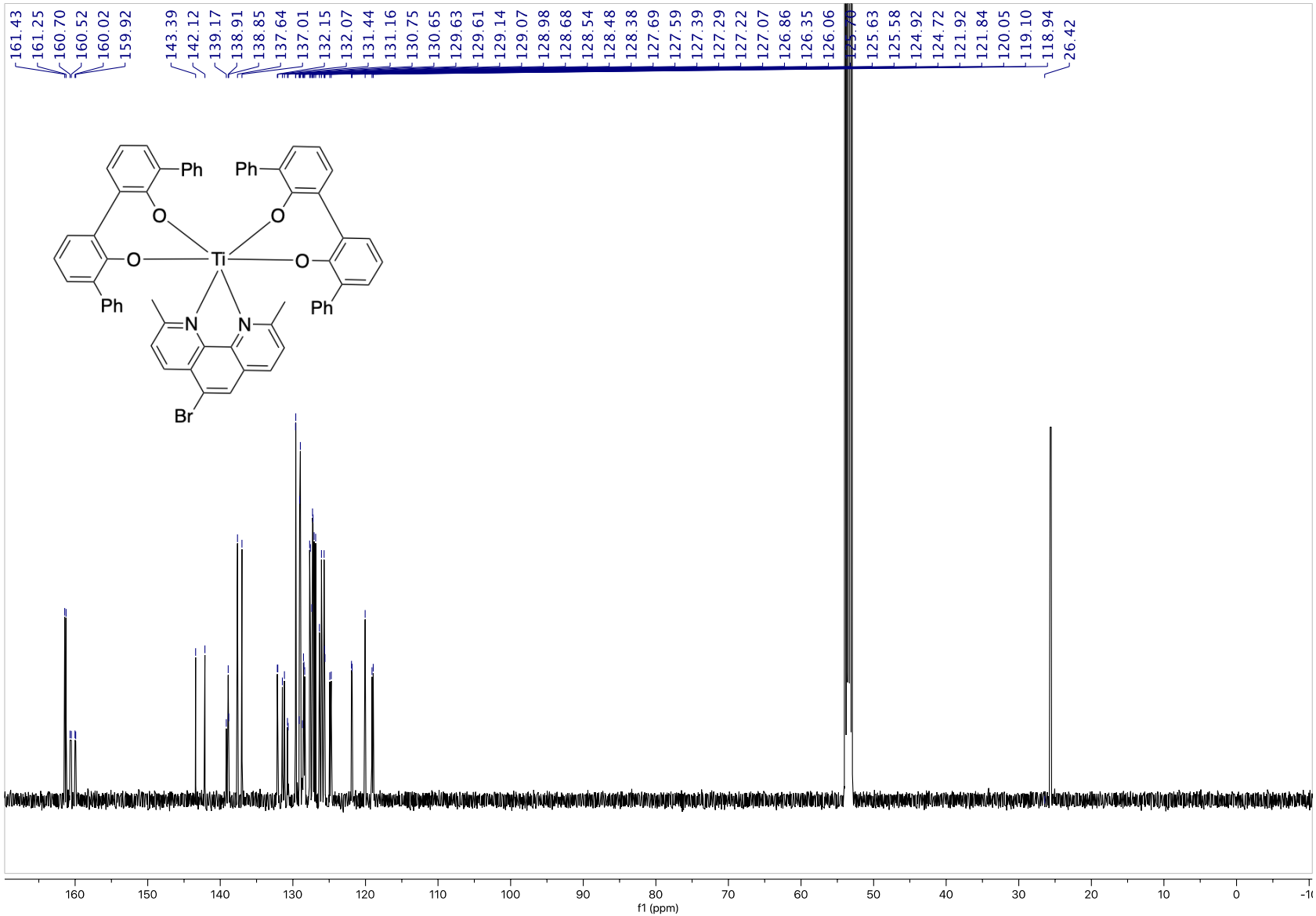


Figure S17: $^{13}C\{^{1}H\}$ NMR spectrum of [Ti(1)$_2$(**2f**)] ($CDCl_3$, 125 MHz)

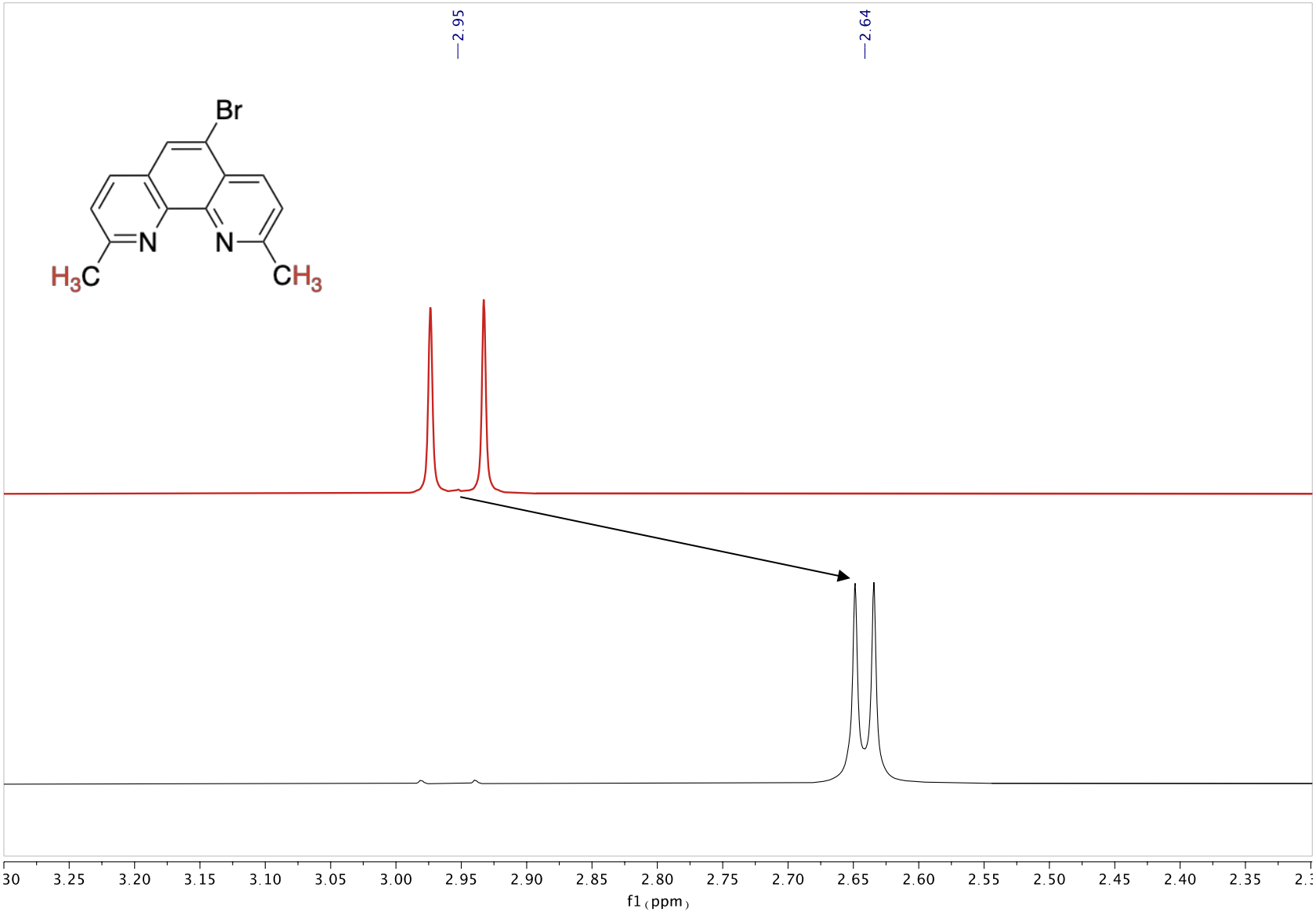


Figure S18: Superposition of the $^{1}H$ NMR spectra of **2f** (top) and [Ti(1)$_2$(**2f**)] (bottom) ($CDCl_3$, 500 MHz)

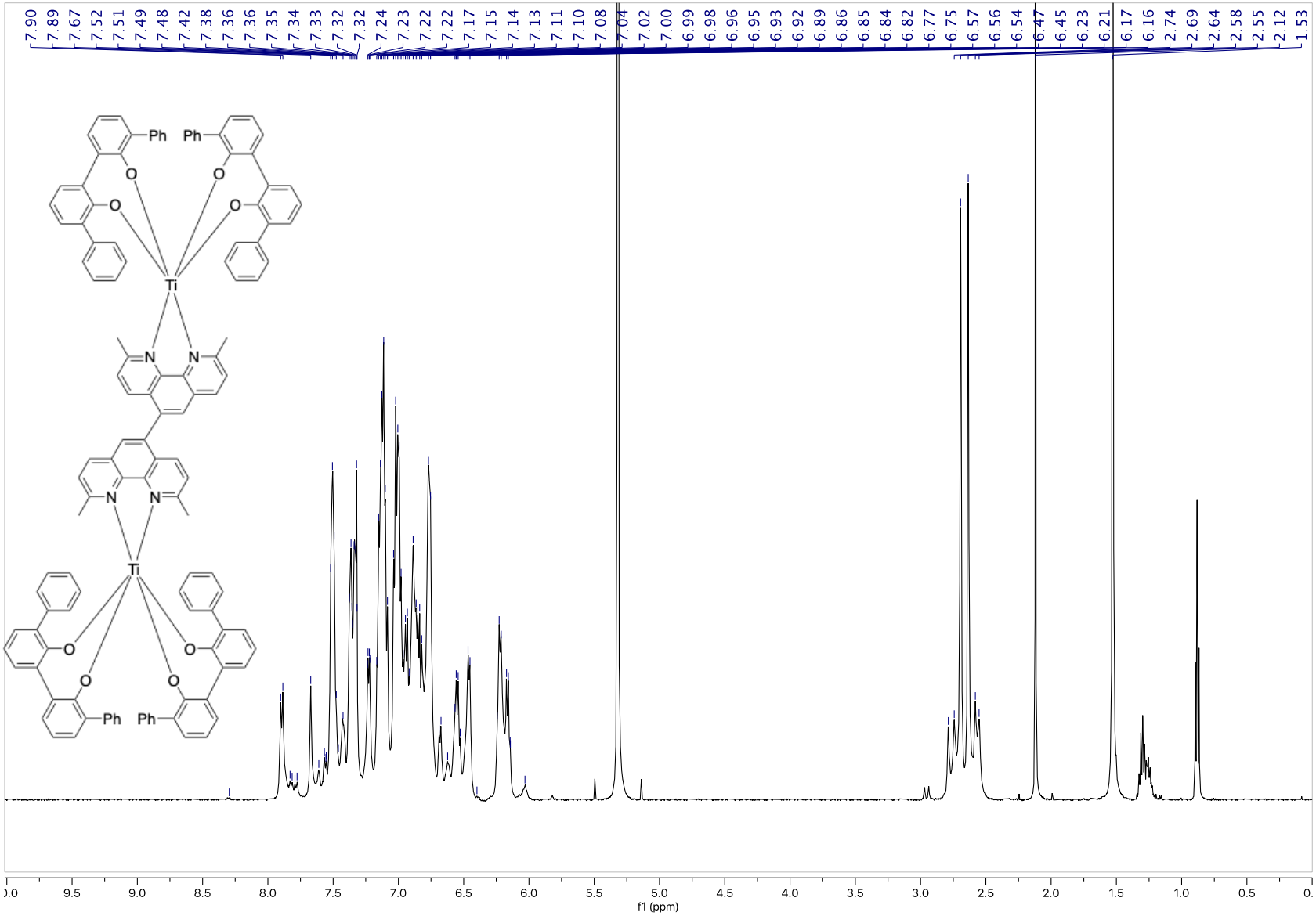


Figure S19: $^{1}H$ NMR spectrum of [Ti(1)$_4$**3**] ($CD_2Cl_2$, 500 MHz)

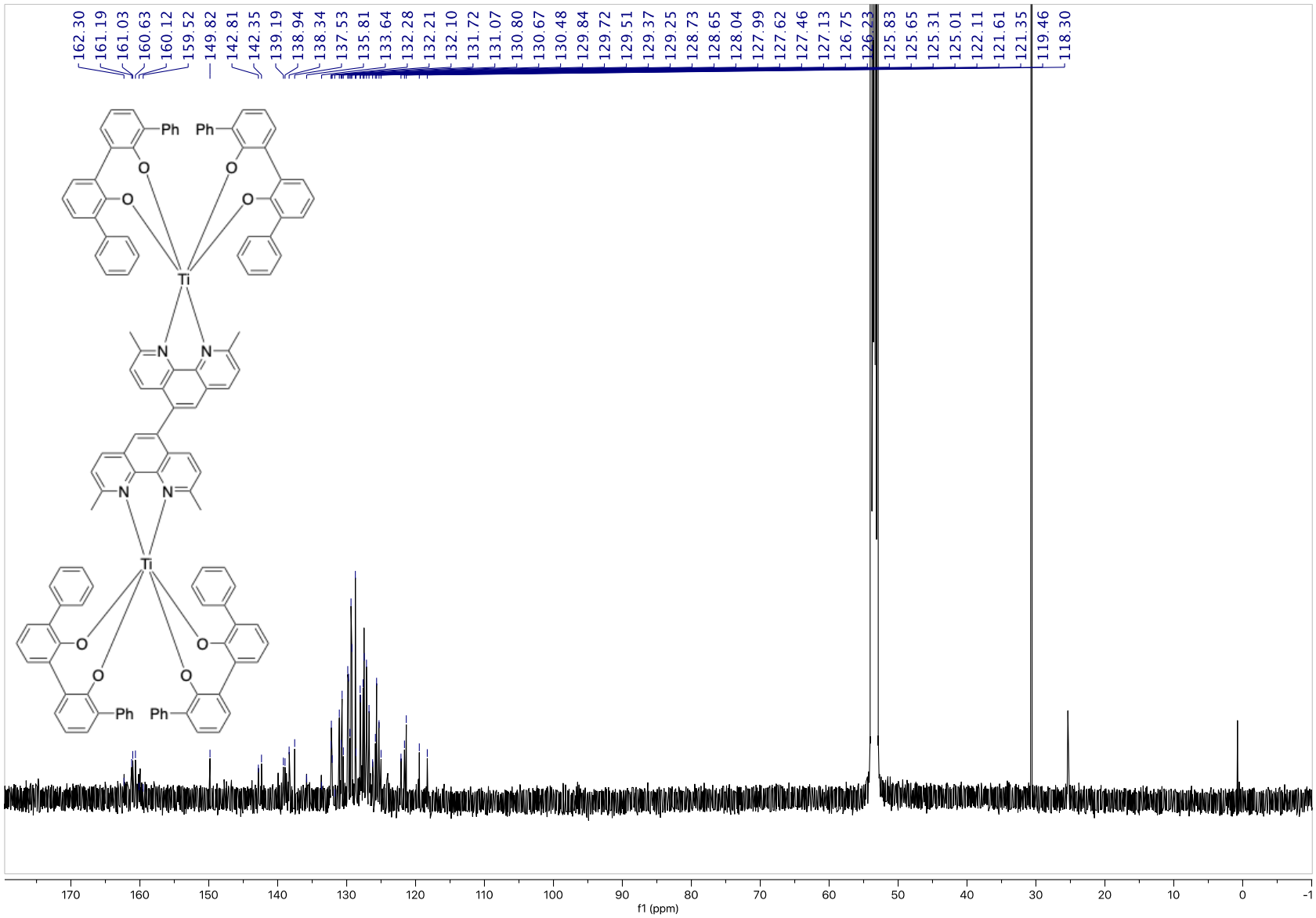


Figure S20: $^{13}C\{^{1}H\}$ NMR spectrum of [Ti(1)$_2$**3**] ($CD_2Cl_2$, 125 MHz)

2. NMR spectra of the hydrolytic stability assay

(●) Ligand signal. (●) Complex signal.

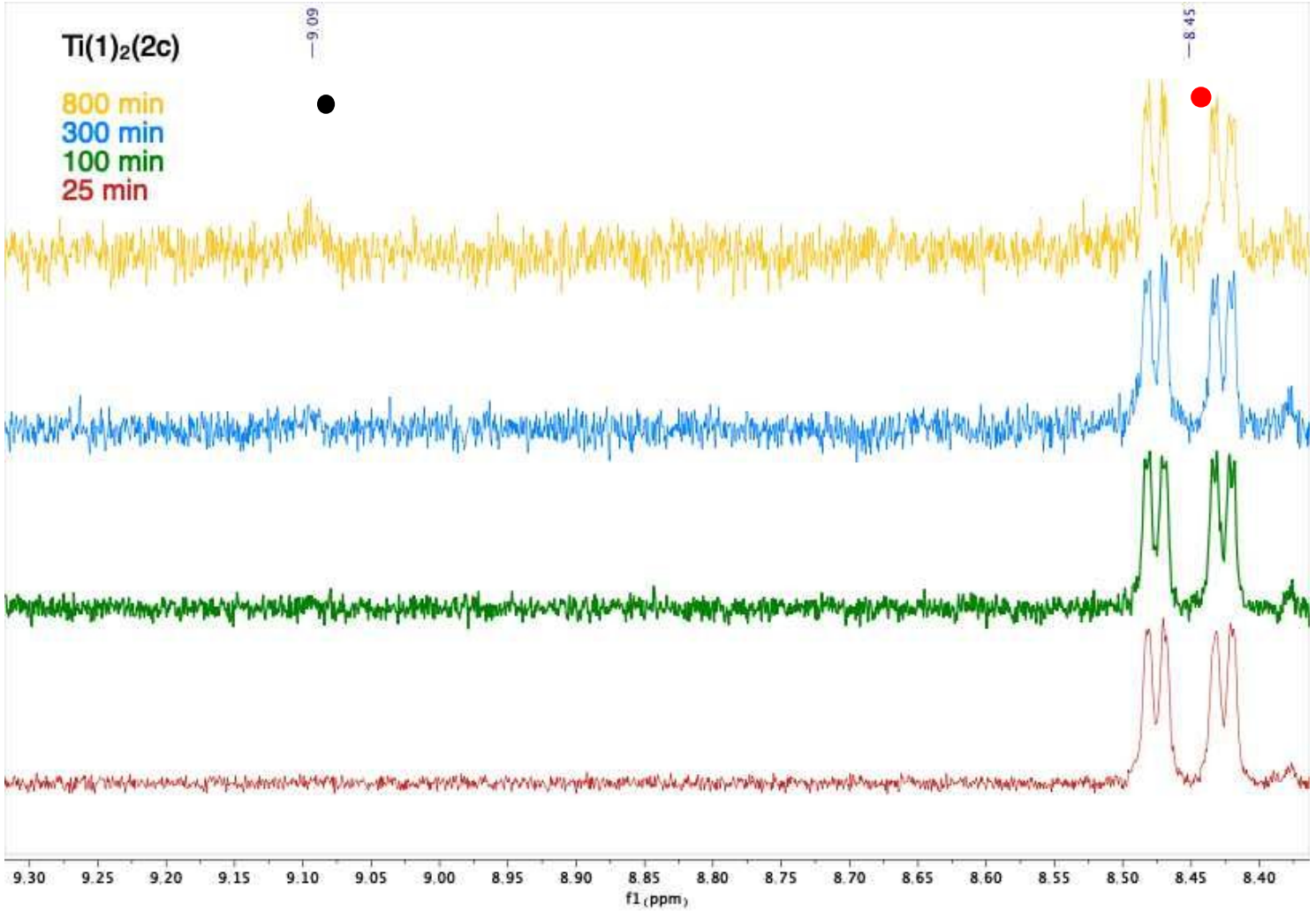


Figure S21: [Ti(1)$_2$(**2c**)]

Figure S22: [Ti(1)$_2$(**2d**)]

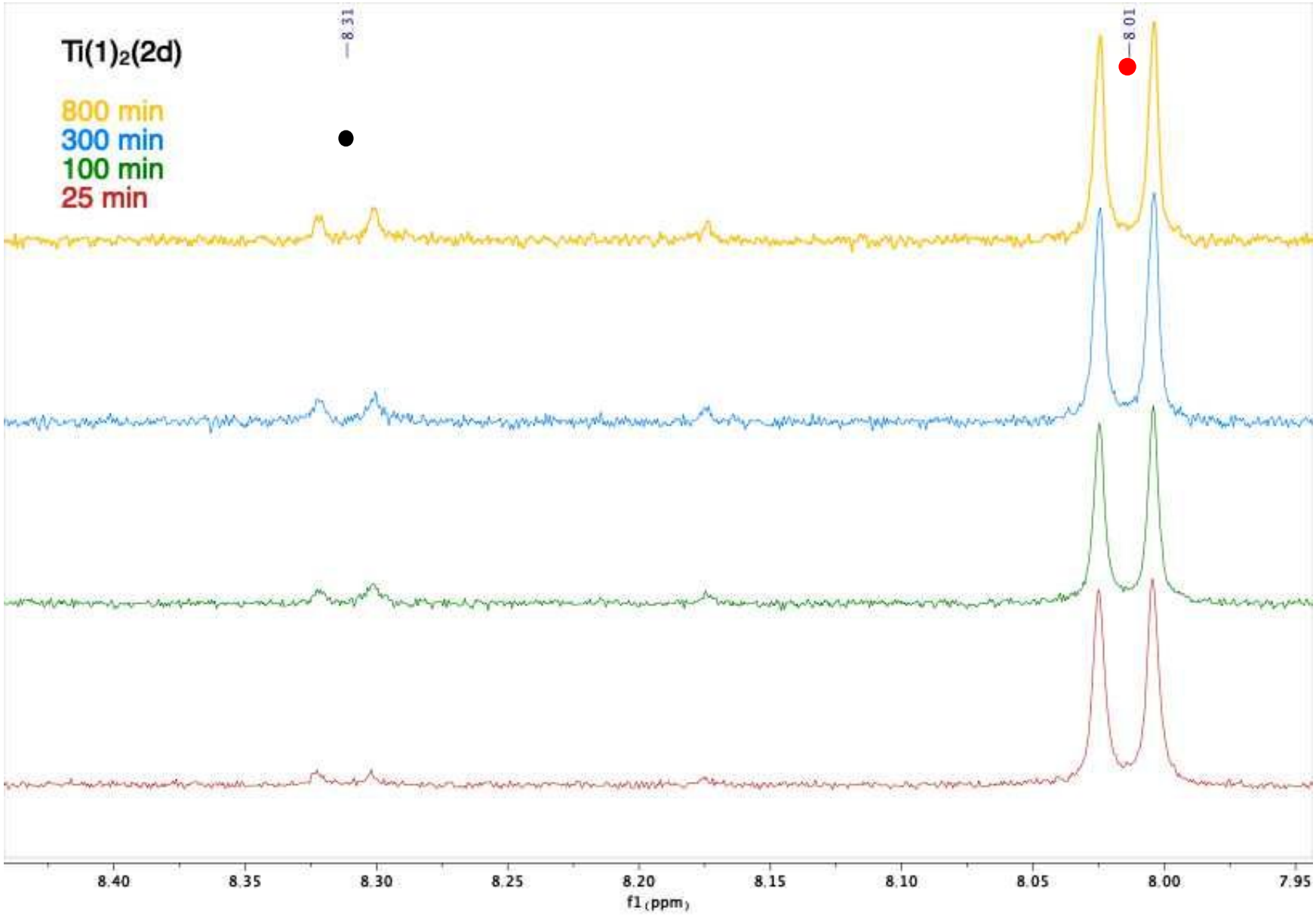

Figure S23: [Ti(1)$_2$(2,2-bipyridine)]

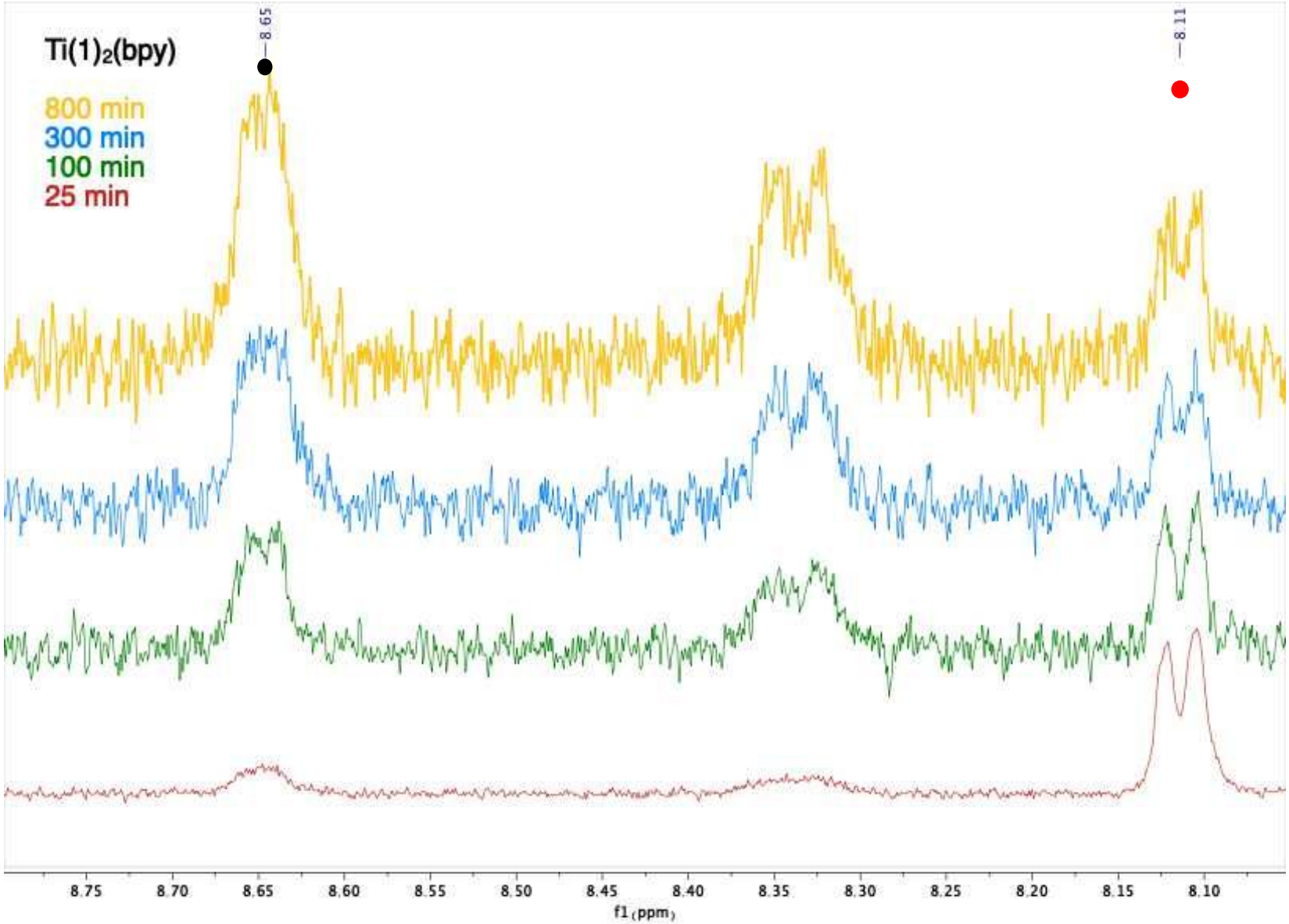

## 2. DFT

Table S1: Selected O-Ti-O and N-Ti-N bond angles and β and α angles measured from the computed minimized structures with the B3LYP functional in the gas phase (rounded values). For a definition of β and α please refer to Figure 1.

| | Angles (°) | | | | |
|---|---|---|---|---|---|
| | N-Ti-N | $O_{ax}$-Ti-$O_{ax}$ | $O_{eq}$-Ti-$O_{eq}$ | β | α |
| [Ti(**1**)$_2$(**2a**)] | 71.5 | 173.7 | 112.4 | 1.9 | 1.6 |
| [Ti(**1**)$_2$(**2b**)] | 71.4 | 172.6 | 112.1 | 2.1 | 1.9 |
| [Ti(**1**)$_2$(**2c**)] | 71.6 | 173.2 | 111.9 | 3.3 | 0.5 |
| [Ti(**1**)$_2$(**2d**)] | 72.1 | 169.9 | 104.1 | 9.3 | 10.5 |
| [Ti(**1**)$_2$(**2e**)] | 72.3 | 169.5 | 100.3 | 9.9 | 9.8 |
| [Ti(**1**)$_2$(**2f**)] | 72.7 | 169.0 | 101.8 | 11.1 | 10.9 |

Table S2: Main characteristics of the 6 lowest energy transition in the various complexes obtained via DFT calculations in the gas phase or in $CH_2Cl_2$.

| | | 1 | 2 | 3 | 4 | 5 | 6 |
|---|---|---|---|---|---|---|---|
| GAS PHASE | | | | | | | |
| [Ti(**1**)$_2$(**2a**)] | ΔE (eV / nm) | 2.2241 / 557 | 2.2310 / 556 | 2.4377 / 509 | 2.4477 / 507 | 2.4652 / 503 | 2.5734 / 482 |
| | Osc-Strength | 0.0042 | 0.0000 | 0.0027 | 0.0026 | 0.0014 | 0.0006 |
| [Ti(**1**)$_2$(**2b**)] | ΔE (eV / nm) | 2.1715 / 571 | 2.1766 / 570 | 2.3302 / 532.07 | 2.3403 / 530 | 2.3817 / 521 | 2.5115 / 494 |
| | Osc-Strength | 0.0036 | 0.0001 | 0.0026 | 0.0023 | 0.0003 | 0.0005 |
| [Ti(**1**)$_2$(**2c**)] | ΔE (eV / nm) | 2.2509 / 551 | 2.2574 / 549 | 2.4568 / 505 | 2.4583 / 504 | 2.4778 / 500 | 2.5962 / 478 |
| | Osc-Strength | 0.0040 | 0.0004 | 0.0038 | 0.0036 | 0.0003 | 0.0006 |
| [Ti(**1**)$_2$(**2d**)] | ΔE (eV / nm) | 2.4247 / 511 | 2.5878 / 479 | 2.6735 / 464 | 2.7599 / 449 | 2.7921 / 444 | 2.8204 / 440 |
| | Osc-Strength | 0.0010 | 0.0048 | 0.0136 | 0.0169 | 0.0036 | 0.0033 |
| [Ti(**1**)$_2$(**2e**)] | ΔE (eV / nm) | 2.4240 / 512 | 2.5173 / 493 | 2.6567 / 467 | 2.6658 / 465 | 2.7533 / 450 | 2.7865 / 445 |
| | Osc-Strength | 0.0017 | 0.0021 | 0.0092 | 0.0079 | 0.0038 | 0.0008 |
| [Ti(**1**)$_2$(**2f**)] | ΔE (eV / nm) | 2.3705 / 523 | 2.4964 / 497 | 2.602 / 476 | 2.6914 / 461 | 2.7078 / 458 | 2.7243 / 455 |
| | Osc-Strength | 0.0003 | 0.0029 | 0.0071 | 0.0015 | 0.0065 | 0.0031 |
| $CH_2Cl_2$ | | | | | | | |
| [Ti(**1**)$_2$(**2a**)] | ΔE (eV / nm) | 2.5650 / 483 | 2.5957 / 478 | 2.7341 / 453 | 2.7688 / 448 | 2.8381 / 437 | 2.9441 / 421 |
| | Osc-Strength | 0.0002 | 0.0119 | 0.0203 | 0.0050 | 0.0010 | 0.0018 |
| [Ti(**1**)$_2$(**2b**)] | ΔE (eV / nm) | 2.4973 / 496 | 2.5308 / 490 | 2.6697 / 464 | 2.7036 / 459 | 2.7611 / 449 | 2.8340 / 437 |
| | Osc-Strength | 0.0001 | 0.0104 | 0.0123 | 0.0048 | 0.0001 | 0.0084 |
| [Ti(**1**)$_2$(**2c**)] | ΔE (eV / nm) | 2.5637 / 484 | 2.5968 / 477 | 2.7240 / 455 | 2.7624 / 449 | 2.8353 / 437 | 2.9187 / 425 |
| | Osc-Strength | 0.0002 | 0.0114 | 0.0208 | 0.0063 | 0.0009 | 0.0023 |
| [Ti(**1**)$_2$(**2d**)] | ΔE (eV / nm) | 2.6396 / 470 | 2.7651 / 448 | 2.8606 / 433 | 2.8847 / 430 | 3.0279 / 409 | 3.0351 / 409 |
| | Osc-Strength | 0.0034 | 0.0372 | 0.0206 | 0.0027 | 0.0070 | 0.0080 |
| [Ti(**1**)$_2$(**2e**)] | ΔE (eV / nm) | 2.6600 / 466 | 2.762 / 449 | 2.8029 / 442 | 2.9054 / 442 | 2.9678 / 418 | 3.043 / 407 |
| | Osc-Strength | 0.0125 | 0.0309 | 0.0014 | 0.0014 | 0.0162 | 0.0063 |

| | | | | | | | |
|---|---|---|---|---|---|---|---|
| [Ti(**1**)$_2$(**2f**)] | ΔE (eV / nm) | 2.6198 / 473 | 2.7445 / 452 | 2.7668 / 448 | 2.8809 / 430 | 2.9571 / 419 | 2.9798 / 416 |
| | Osc-Strength | 0.0061 | 0.0380 | 0.0070 | 0.0021 | 0.0026 | 0.0087 |

Figure S24: Computed visible spectra, calculations made for complexes in a $CH_2Cl_2$ solution (left) and in a gas phase (right)

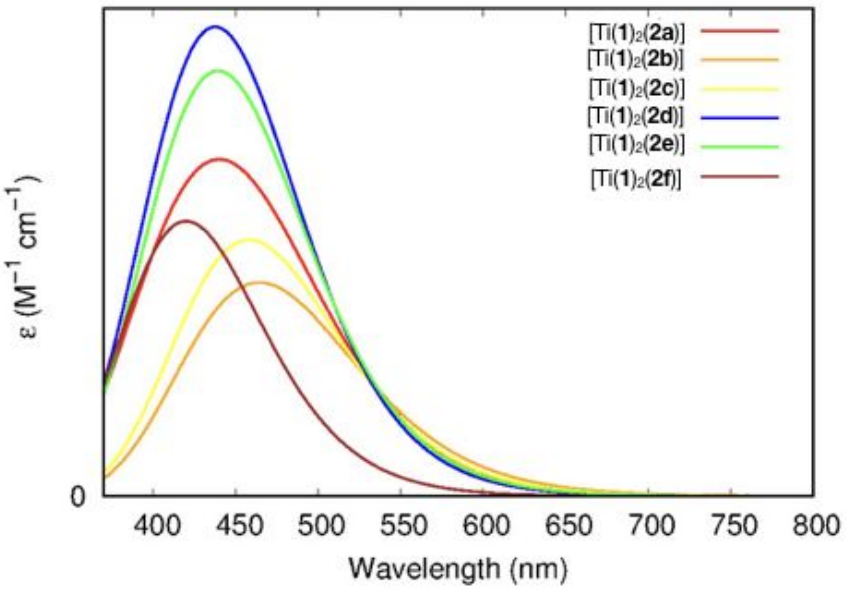
[Ti(1)2(2a)]
[Ti(1)2(2b)]
[Ti(1)2(2c)]
[Ti(1)2(2d)]
[Ti(1)2(2e)]
[Ti(1)2(2f)]
ε (M−1 cm−1)
0
400 450 500 550 600 650 700 750 800
Wavelength (nm)

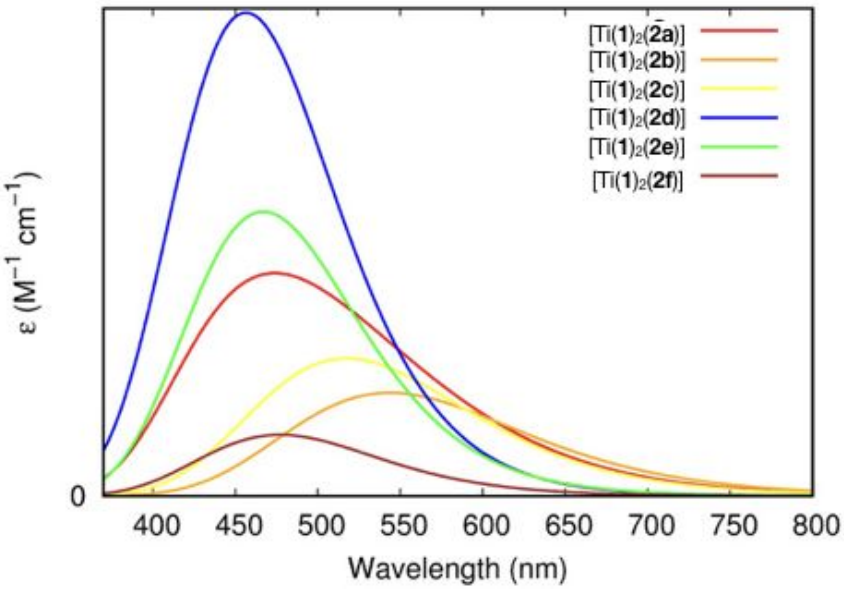
[Ti(1)2(2a)]
[Ti(1)2(2b)]
[Ti(1)2(2c)]
[Ti(1)2(2d)]
[Ti(1)2(2e)]
[Ti(1)2(2f)]
ε (M−1 cm−1)
0
400 450 500 550 600 650 700 750 800
Wavelength (nm)

**Figure S25:** Representation of the occupied and unoccupied molecular orbitals involved in the transition of highest intensity in the Gas Phase.

| | Occupied Orbitals | Unoccupied Orbitals |
|---|---|---|
| [Ti(**1**)$_2$(**2a**)] | 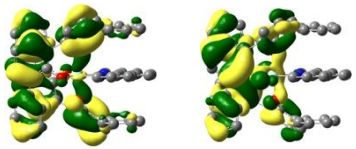 | 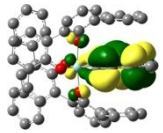 |
| [Ti(**1**)$_2$(**2b**)] | 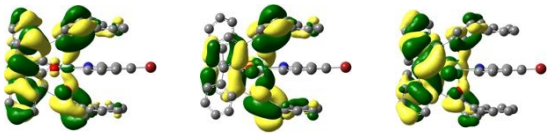 |  |
| [Ti(**1**)$_2$(**2c**)] | 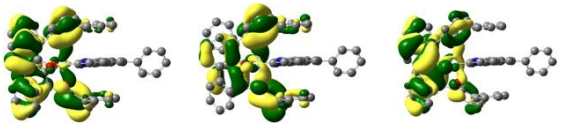 | 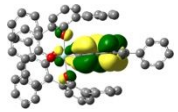 |
| [Ti(**1**)$_2$(**2d**)] | 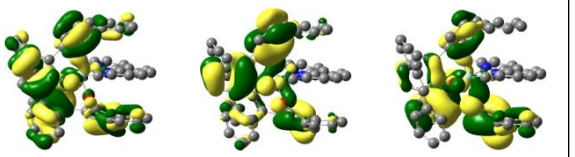 | 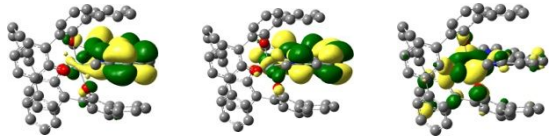 |
| [Ti(**1**)$_2$(**2e**)] | 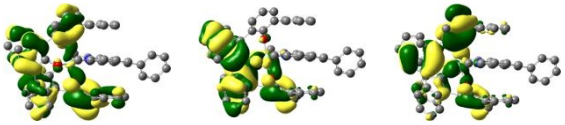 | 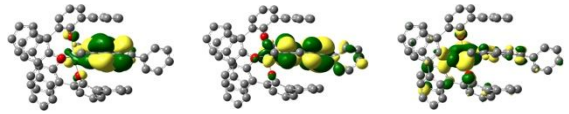 |

| | | |
|---|---|---|
| [Ti(**1**)$_2$(**2f**)] | 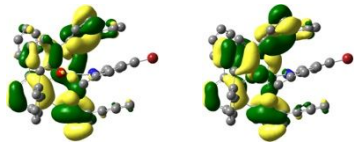 | 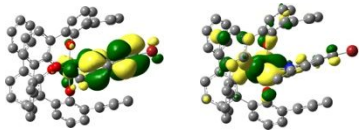 |

**Figure S26:** Representation of the occupied and unoccupied molecular orbitals involved in the transition of highest intensity in the $CH_2Cl_2$.

| | Occupied Orbitals | Unoccupied Orbitals |
|---|---|---|
| [Ti(**1**)$_2$(**2a**)] | 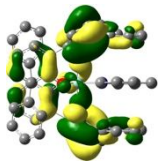 | 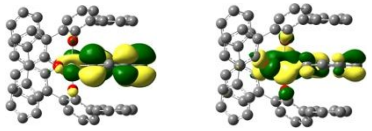 |
| [Ti(**1**)$_2$(**2b**)] | 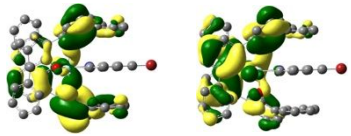 | 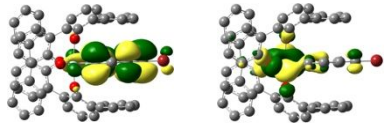 |
| [Ti(**1**)$_2$(**2c**)] | 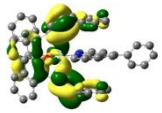 | 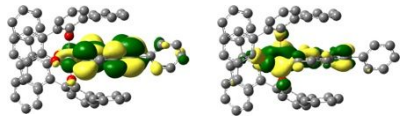 |
| [Ti(**1**)$_2$(**2d**)] | 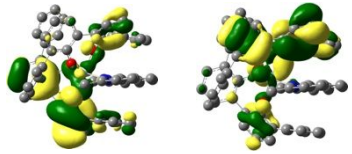 | 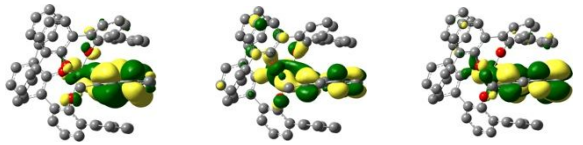 |

| | | | | | |
|---|---|---|---|---|---|
| [Ti(**1**)$_2$(**2e**)] | 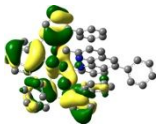 | 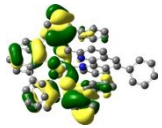 |  | 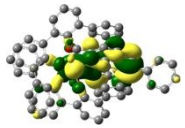 | 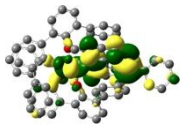 |
| [Ti(**1**)$_2$(**2f**)] | 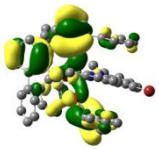 | 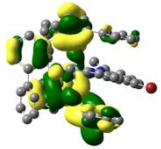 |  | 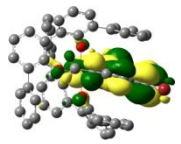 | 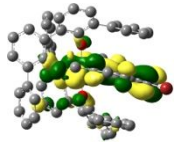 |

## 3. UV-visible spectra (experimental)

Figure S27: Liquid UV-Visible spectra for [Ti(1)($2_2$**a-f**)] and [Ti$(1)_{4k}$**(2K)**]